Analytical Other-Cell Interference Characterization over HSUPA-Enabled Multi-cell UMTS Networks

Tuo Liu
School of Information Technologies
University of Sydney, NSW 2006, Australia
Email: tliu@it.usyd.edu.au

Andreas Mäder and Dirk Staehle
Department of Distributed Systems, University of Würzburg
Am Hubland, D-97074 Würzburg, Germany
Email: {maeder,staehle}@informatik.uni-wuerzburg.de

Abstract—**In this paper we present an analytical model for deriving the other-cell interference distribution in the multi-cell UMTS with recent evolvement, high speed uplink packet access, enabled. Fixed-point equations are employed for iteratively computing the distribution, and log-normal approximations are suggested to increase the efficiency of algorithms significantly. The accuracy of the approximation is further enhanced with certain techniques. The accuracy of analytical model is then verified through the comparisons with simulation results, where good matches are achieved implying the possibility of application in practical network planning.**

I. INTRODUCTION

The UMTS is the European standard of 3G mobile telecommunications systems with WCDMA as its air interface. The performance of packet access in UMTS keeps improving, firstly by the introduction of HSDPA (High-Speed Downlink Packet Access) [1] in Release 5 for increasing bandwidth demands in the downlink direction, and then recently with the proposal of HSUPA (High-Speed Uplink Packet Access) [2] in Release 6 to meet the growing traffic requests in the uplink direction. Three new major features are employed in the UMTS HSUPA in order to fulfill the higher bandwidth requirements, which are *fast hybrid ARQ*, *fast scheduling* implemented in NodeB and *short TTI* (Transmission Time Interval) of 2ms [3]. Among these features, the relocation of the scheduler from RNC (Radio Network Controller) to NodeB allows much more rapidity and flexibility for the implementation of RRM (Radio Resource Management).

The analytical models for the interference in conventional QoS traffic-only systems operating with either target SIR (Signal-to-Interference-Ratio) oriented RRM [4] [5] [6] or target received power oriented RRM [7] [8] have been intensively studied. Moreover, much effort has been spent on the interference model construction and performance analysis for the QoS/best-effort data integrated multi-service CDMA systems [9] [10] and recent 3G networks [11]. For the newly evolved HSUPA-enabled 3G systems, analytical interference and load models are proposed in [12] to give the blocking probability, cell load and bit rate. However, this paper only accounts for the single-cell scenarios since the other-cell interference is simply assumed as an independent random variable.

In this work, we extend the analysis on the base of [6] and [12] to present an analytical model for the other-cell interfer-

ence characterization in multi-cell environments. Unlike the previous assumption that interference levels in each cell are totally independent, in practice, a fluctuation in the other-cell interference level of a certain cell results in corresponding varying of the transmission power of all the UEs (User Equipments) in such cell, which then influences the other-cell interference received at each NodeB in all the other cells and again that in the reference cell. These interactions among cells are defined as feedback behavior in [4], which makes the modeling task not straightforward any more, and most previous studies on best-effort traffic supported systems do not take this factor into account. In order to capture the feedback behavior, we formulate the other-cell interferences with fixed-point equations, and solve them by iterative approach. Furthermore, to avoid the numerous convolutions which are involved in the direct distribution derivation, log-normal approximations are suggested with further enhancement of the accuracy of approximation discussed.

The rest of this paper is organized as follows. In section II, the distributed RRM for HSUPA-enabled UMTS is described. Section III demonstrates the uplink interference model with deterministic user patterns. while section IV derives the stochastic model with random user patterns. Also in section IV, a log-normal approximation approach is described with an accuracy enhancement technique to capture the effects of interference feedback. Both simulation results from Monte-Carlo simulations and numerical results from analytical models are illustrated in section V to verify the suggested analytical approximation approach. The paper is concluded in section VI, and the scope for future work is highlighted.

II. ON THE RADIO RESOURCE MANAGEMENT FOR HSUPA

The employed RRM plays an important role in the system behaviors, and in turn for the other-cell interference. Therefore, before going into the interference model construction, we explain in this section the resource management schemes such as blocking criteria, rate allocation algorithm, etc., which are used for the later proposed analytical model. One major advance of HSUPA compared with the conventional uplink is the fast scheduling, which allows the resources for UEs to be allocated at each individual NodeB, rather than at the RNC in previous releases. A new MAC (Medium Access Control) entity has been introduced in each NodeB for this purpose,

thus the RRM algorithms employed in HSUPA become decentralized, which differs most from that of classical UMTS uplinks, and accordingly affects the interference model.

In the UMTS uplink, the shared resource is the interference power received at NodeB, which normally depends on the user data rate, the target bit-energy-to-interference-ratio, etc. In [13], a new term 'cell load', which can be uniquely determined by the received interference, is introduced and the load η_x in cell x is defined as

$$\eta_x = \frac{I_x}{I_x + WN_0} \tag{1}$$

where I_x is the received interference at NodeB x from all the DCH (Dedicated Channel) and E-DCH (Enhanced Dedicated Channel) users over the system, W is the system bandwidth and N_0 is the background noise density. The received interference consists of power from DCH users and E-DCH users in own cell and other cells (i.e. $I_x = I_{x,own}^D + I_{x,own}^E + I_{x,oc}^D + I_{x,oc}^E$), hence the cell load can be consequently decomposed into four corresponding parts according to different sources ($\eta_{x,own}^D, \eta_{x,own}^E, \eta_{x,oc}^D$ and $\eta_{x,oc}^E$). The data rates of E-DCH users can be easily determined from the own-cell load based on some equations introduced in the next section, thus the essence of rate allocation translates into the own-cell load evaluation.

In our analytical model, we further assume that rate allocation performed only with local load information, which aims to keep the own-cell received load as own-cell target load η_{own}^* by adjusting $\eta_{x,own}^E$

$$\eta_{x,own} = \eta_{x,own}^D + \eta_{x,own}^E = \eta_{own}^*. \tag{2}$$

The other-cell interference under such strategy can be analytically characterized with known PDF being a function of own-cell target load η_{own}^* by techniques introduced later in this paper. The network capacity can be then easily analyzed and adjusted with the parameter η_{own}^* from such a model.

Note that even though RRM does not consider the interference from other cells, interference levels at different NodeBs still depend on each other during operation due to the feedback behavior, which is the key point in the analysis. Also with such 'waterfilling' radio resource management, the above equation always holds unless there is no E-DCH user in the current cell, where $\eta_{x,own}$ is simply equal to $\eta_{x,own}^D$ that cannot be adjusted by rate allcation.

The own-cell target load η_{own}^* also serves as a reference for admission control in the RRM. If the received load from own-cell DCH users together with the minimum load contributed by own-cell E-DCH users (i.e. each E-DCH user is only allocated R_{min}^E) exceed the threshold η_{own}^*, a *Blocking* event occurs, during which no incoming users can be admitted. Thus η_{own}^* is also an important parameter for the blocking probability.

III. DETERMINISTIC UPLINK INTERFERENCE MODEL IN HSUPA-ENABLED UMTS

From the UMTS uplink power control equation:

$$\varepsilon_k^* = \frac{W}{R_k} \cdot \frac{S_x^k}{I_x^{own} + I_x^{oc} + WN_0 - S_x^k} \tag{3}$$

with target E_b/I_0 value ε_k^*, received power S_x^k and bit rate R_k of UE k at NodeB x, we can solve for S_x^k following similar procedures in [12] as

$$S_x^k = \frac{\omega_k}{1 - \left(\eta_{x,own}^D + \eta_{x,own}^E\right)} \left(I_x^{oc} + WN_0\right) \tag{4}$$

where ω_k is defined as:

$$\omega_k = \frac{\varepsilon_k^* R_k}{W + \varepsilon_k^* R_k}. \tag{5}$$

With above equations, together with the load definition and decomposition, the own-cell load from DCH and E-DCH users can be easily represented again from [12] as follows

$$\eta_{x,own}^D = \sum_{k \in \mathcal{D}_x} \omega_k^D \quad \text{and} \quad \eta_{x,own}^E = \sum_{j \in \mathcal{E}_x} \omega_j^E \tag{6}$$

where $\mathcal{D}_x$ and $\mathcal{E}_x$ refer to all the DCH and E-DCH users controlled by the NodeB x. It can be seen that ω is in essence the effective load contributed by each individual user to its serving NodeB, thus referred to as SLF (*Service Load Factor*).

The rate allocation for each E-DCH user within one cell depends on the employed scheduling discipline. Assuming parallel equal-rate scheduling is employed, then every E-DCH user within one cell shares the same SLF ω_j^E, where the instant ω_j^E is determined from (2),

$$\omega_j^E = \frac{\eta_{own}^* - \eta_{x,own}^D}{n_x^E} \tag{7}$$

where n_y^E refers to the number of E-DCH users in this cell.

So far only the received power from own-cell users is characterized, then to model the other-cell interference, we first investigate the inter-cell received power $S_{y \to x}^k$ at NodeB x, which is the power contributed by one UE k that belongs to the NodeB y. With the same propagation model in [6], if we further assume each UE chooses the NodeB with least attenuation as its serving NodeB, $S_{y \to x}^k$ can be represented as

$$S_{y \to x}^k = S_y^k \Delta_{y \to x}^k \tag{8}$$

where $\Delta_{y \to x}^k$ is used to denote the attenuation ratio $(d_y^k / d_x^k)^\gamma$.

Again we have a similar form of linear equations as in [4]

$$I_x^{oc} = \sum_{y \neq x} I_{y \to x}^{out} \tag{9}$$

$$I_{y \to x}^{out} = \left(I_y^{oc} + WN_0\right) F_{y \to x}, \tag{10}$$

but now they differ from previous work in $F_{y \to x}$, where an additional component for E-DCH traffic is included.

$$F_{y \to x} = \frac{1}{1 - \left(\eta_{y,own}^D + \eta_{y,own}^E\right)} \left[\sum_{k \in \mathcal{D}_y} \omega_k^D \Delta_{y \to x}^k + \sum_{j \in \mathcal{E}_y} \omega_j^E \Delta_{y \to x}^j \right] \tag{11}$$

From above equations, it can be seen that the variable $F_{y \to x}$ in (11), which consists of user population and location information, is independent of I_x^{oc} and $I_{y \to x}^{out}$. If the user pattern is deterministic, all the parameters in (11) would be given and $F_{y \to x}$ becomes a constant. Then (9) and (10) may construct a

system of linear equations with respect to I_x^{oc} with rank equal to the number of NodeBs. The Monte-Carlo simulation can be accordingly applied and the moments of I_x^{oc} are obtained for the verification of analytical model.

IV. STOCHASTIC UPLINK INTERFERENCE MODEL IN HSUPA-ENABLED UMTS

A. Analytical Model Formulation and Direct Approach

The stochastic fixed-point equations representation of (9) and (10) are formulated as

$$\mathcal{I}_x^{oc} = \sum_{y \neq x} \mathcal{I}_{y \to x}^{out} \quad \text{and} \quad \mathcal{I}_{y \to x}^{out} = \left(\mathcal{I}_y^{oc} + WN_0 \right) \mathcal{F}_{y \to x}. \tag{12}$$

where $\mathcal{I}_x^{oc}$, $\mathcal{I}_{y \to x}^{out}$ and $\mathcal{F}_{y \to x}$ are the corresponding random variables. Similar to the system of linear equations in last section, this set of fixed-point equations also have exactly the same structure as those in our previous work [4] with the only exception of $\mathcal{F}_{y \to x}$, which now becomes

$$\mathcal{F}_{y \to x} = \frac{\sum_{t=1}^{T} \omega_{y,t}^D \sum_{k=1}^{n_{y,t}^D} \Delta_{y \to x}^k + \omega_y^E \sum_{j=1}^{n_y^E} \Delta_{y \to x}^j}{1 - \left(\eta_{y,own}^D + \eta_{y,own}^E \right)} \tag{13}$$

where $n_{y,t}^D$ refers to the number of DCH users of class t in cell y. Therefore, the task now reduces to the characterization of the distribution of $\mathcal{F}_{y \to x}$ in our current model, and then we can apply the same approach for the distribution of other-cell interference.

If the number of users in each class is fixed as $\hat{n}_y^D$ and $\hat{n}_y^E$ in the above expression where $\hat{n}_y^D$ stands for the vector $\left(\hat{n}_{y,1}^D, \ldots, \hat{n}_{y,T}^D \right)$, the values of $\eta_{y,own}^D$, $\eta_{y,own}^E$, $\omega_{y,t}^D$ and ω_y^E can be easily determined from (5)-(7). Then together with the PDF of $\Delta_{y \to x}$ that is approximated in closed form in [6] [8], the conditional PDF $P \left(\mathcal{F}_{y \to x} \leq z | \hat{n}_y^D, \hat{n}_y^E \right)$ can be derived in theory. Finally for the complete PDF of $\mathcal{F}_{y \to x}$, we apply the total probability theorem to uncondition $P \left(\mathcal{F}_{y \to x} \leq z | \hat{n}_y^D, \hat{n}_y^E \right)$ as

$$P \left(\mathcal{F}_{y \to x} \leq z \right) = \sum_{\hat{n}_y^D, \hat{n}_y^E \in \mathbf{S}} P(\hat{n}_y^D, \hat{n}_y^E) \cdot P \left(\mathcal{F}_{y \to x} \leq z | \hat{n}_y^D, \hat{n}_y^E \right) \tag{14}$$

where the user distribution $P(\hat{n}_y^D, \hat{n}_y^E)$ is given according to a spatial homogeneous Poisson process [14] as a product form

$$P(\hat{n}_y^D, \hat{n}_y^E) = P_0 \cdot \frac{\left(N_y^E \right)^{\hat{n}_y^E}}{\hat{n}_y^E!} \prod_{t=1}^{T} \frac{\left(N_{y,t}^D \right)^{\hat{n}_{y,t}^D}}{\hat{n}_{y,t}^D!} \tag{15}$$

where $N_{y,t}^D$ denotes the mean number of DCH users of class t, N_y^E refers to that of E-DCH users and P_0 is the normalizing constant. The admissible region $\mathbf{S}$ is defined by the admission control policy suggested in the previous section, where the sum of own-cell DCH load and minimum E-DCH load cannot exceed own-cell target load η_{own}^*

$$\hat{n}_y^D, \hat{n}_y^E \in \mathbf{S} \quad \text{if} \quad \hat{n}_y^E \omega_{min}^E + \sum_{t=1}^{T} \hat{n}_{y,t}^D \omega_{y,t}^D < \eta_{own}^*. \tag{16}$$

Theoretically, with all the acquired PDFs of the random variables above, the PDF of $\mathcal{F}_{y \to x}$ can be obtained, however, it is quite a hard task due to the involvement of numerous convolutions which is in fact numerical intractable. Thus we will investigate some approximation techniques in the next section to reduce the computational complexity. For the same reason, the approximation approach is employed for the other-cell interference $\mathcal{I}_x^{oc}$ as well.

B. Log-normal Approximation Approach

In order to avoid the extremely time-consuming computation for the PDF derivation of $\mathcal{I}_x^{oc}$, we propose an efficient approximation technique in light of the excellent log-normal approximation of other-cell interference in QoS traffic only UMTS in [4] [6]. Through similar verification experiments but with additional best-effort traffic, both $\mathcal{F}_{y \to x}$ and $\mathcal{I}_x^{oc}$ are still shown to be well approximated by the log-normal distribution. This reduces the problem to determining only the first and second moments of both random variables.

Again by the total probability theorem, the first moment of $\mathcal{F}_{y \to x}$ is given as

$$E \left[\mathcal{F}_{y \to x} \right] = \sum_{\hat{n}_y^D \in \mathbf{S}, \hat{n}_y^E = 0} P(\hat{n}_y^D, 0) \frac{\eta_{y,own}^D}{1 - \eta_{y,own}^D} E \left[\Delta_{y \to x} \right]$$
$$+ \sum_{\hat{n}_y^D, \hat{n}_y^E \in \mathbf{S} \backslash (\hat{n}_y^E = 0)} P(\hat{n}_y^D, \hat{n}_y^E) \frac{\eta_{own}^*}{1 - \eta_{own}^*} E \left[\Delta_{y \to x} \right] \tag{17}$$

and the second moment is

$$E \left[\mathcal{F}_{y \to x}^2 \right] = \sum_{\hat{n}_y^D, \hat{n}_y^E \in \mathbf{S}} P(\hat{n}_y^D, \hat{n}_y^E) \left(VAR \left[\mathcal{F}_{y \to x} \left(\hat{n}_y^D, \hat{n}_y^E \right) \right] \right.$$
$$\left. + E \left[\mathcal{F}_{y \to x} \left(\hat{n}_y^D, \hat{n}_y^E \right) \right]^2 \right) \tag{18}$$

where $\mathcal{F}_{y \to x} \left(\hat{n}_y^D, \hat{n}_y^E \right)$ denotes the random variable $\mathcal{F}_{y \to x}$ conditioned on known particular user combination. The conditional variance is calculated as

$$VAR \left[\mathcal{F}_{y \to x} \left(\hat{n}_y^D, \hat{n}_y^E \right) \right] = \sum_{\hat{n}_y^D \in \mathbf{S}, \hat{n}_y^E = 0} P(\hat{n}_y^D, 0) \cdot VAR \left[\Delta_{y \to x} \right]$$
$$\cdot \frac{\sum_{t=1}^{T} \hat{n}_{y,t}^D \left(\omega_{y,t}^D \right)^2}{\left(1 - \eta_{y,own}^D \right)^2} + \sum_{\hat{n}_y^D, \hat{n}_y^E \in \mathbf{S} \backslash (\hat{n}_y^E = 0)} P(\hat{n}_y^D, \hat{n}_y^E) \cdot VAR \left[\Delta_{y \to x} \right]$$
$$\cdot \frac{\sum_{t=1}^{T} \hat{n}_{y,t}^D \left(\omega_{y,t}^D \right)^2 + \frac{1}{\hat{n}_y^E} \left(\eta_{own}^* - \eta_{y,own}^D \right)^2}{\left(1 - \eta_{own}^* \right)^2}. \tag{19}$$

To calculate $E[\Delta_{y \to x}]$ and $VAR[\Delta_{y \to x}]$ that appear in the above expressions, we simply follow the same procedure in [6] with the approximated PDF of $\Delta_{y \to x}$. Altogether, the moments of $\mathcal{F}_{y \to x}$ are thus computed. Once $\mathcal{F}_{y \to x}$ is characterized, with the assumption of mutual independence between $\mathcal{F}_{y \to x}$ and $\mathcal{I}_y^{oc}$ as well as among $\mathcal{I}_{y \to x}^{out}$, the first and second moments of the other-cell interference can be derived by iterative method in [4] or by direct matrix equation solving in [15].

C. Accuracy Enhancement of the Approximation

In the derivation above, we made the assumption of complete independence between $\mathcal{F}_{y \to x}$ and $\mathcal{I}_y^{oc}$. However, due to the feedback behavior caused by mutual influences among transmission power of all the UEs, the correlation between these two random variables cannot be neglected, thus introduces some errors in the suggested analytical model. In this section, we try to investigate how to alleviate such errors.

If the dependence between $\mathcal{F}_{y \to x}$ and $\mathcal{I}_y^{oc}$ is considered, the first moment of $\mathcal{I}_x^{oc}$ should be written as

$$E\left[\mathcal{I}_x^{oc}\right] = \sum_{y \neq x} \left[W N_0 \cdot E\left[\mathcal{F}_{y \to x}\right] + E\left[\mathcal{I}_y^{oc}\right] E\left[\mathcal{F}_{y \to x}\right] \right. \\ \left. \cdot \left(1 + \mathcal{G}_{\mathcal{I}_y^{oc}, \mathcal{F}_{y \to x}}\right) \right] \quad (20)$$

with a new function $\mathcal{G}$ introduced, which is defined as

$$\mathcal{G}_{x,y} = c_x \cdot c_y \cdot \rho_{x,y} \quad (21)$$

where c_x, c_y are the coefficients of variation of x and y, and $\rho_{x,y}$ is the correlation coefficient between these two random variables. If we determine the value of $\mathcal{G}_{\mathcal{I}_y^{oc}, \mathcal{F}_{y \to x}}$ from the Monte-Carlo simulation, the modified mean of other-cell interference can be accordingly calculated.

Similarly, for the second moment, it can be represented as

$$E\left[\left(\mathcal{I}_x^{oc}\right)^2\right] = \hat{\mathcal{H}}_x + \sum_{y \neq x} E\left[\left(\mathcal{I}_y^{oc}\right)^2\right] E\left[\mathcal{F}_{y \to x}^2\right] \\ \cdot \left(1 + \mathcal{G}_{\left(\mathcal{I}_y^{oc}\right)^2, \mathcal{F}_{y \to x}^2}\right) \quad (22)$$

where

$$\hat{\mathcal{H}}_x = E\left[\mathcal{I}_x^{oc}\right]^2 + \sum_{y \neq x} \left[(W N_0)^2 \cdot E\left[\mathcal{F}_{y \to x}^2\right] + 2 W N_0 \cdot E\left[\mathcal{I}_y^{oc}\right] \right. \\ \left. \cdot E\left[\mathcal{F}_{y \to x}^2\right] \left(1 + \mathcal{G}_{\mathcal{I}_y^{oc}, \mathcal{F}_{y \to x}^2}\right) \right] - \sum_{y \neq x} \left[W N_0 \cdot E\left[\mathcal{F}_{y \to x}\right] \right. \\ \left. + E\left[\mathcal{I}_y^{oc}\right] E\left[\mathcal{F}_{y \to x}\right] \left(1 + \mathcal{G}_{\mathcal{I}_y^{oc}, \mathcal{F}_{y \to x}}\right) \right]^2, \quad (23)$$

which can be solved following the same approach in previous, with the values of $\mathcal{G}_{\mathcal{I}_y^{oc}, \mathcal{F}_{y \to x}}$, $\mathcal{G}_{\mathcal{I}_y^{oc}, \mathcal{F}_{y \to x}^2}$ and $\mathcal{G}_{\left(\mathcal{I}_y^{oc}\right)^2, \mathcal{F}_{y \to x}^2}$ given from simulations.

It can be seen that if we can determine function $\mathcal{G}$ analytically, the accuracy enhancement can be performed in a total analytic way. Taking the first moment derivation as an example, $c_{\mathcal{F}_{y \to x}}$ is given in previous section, and $c_{\mathcal{I}_y^{oc}}$ can be iterative computed since (20) can be regarded as a fixed-point equation, thus the only part undetermined is the correlation coefficient $\rho_{\mathcal{I}_y^{oc}, \mathcal{F}_{y \to x}}$, on which more investigation should be devoted in the future.

V. NUMERICAL RESULTS

For numerical tractability, we consider an area with two-tier hexagonal cell rings surrounding one central cell, thus 19 NodeBs in total. Two service categories are supported in the system, which are one DCH user class with $R_D = 12.2\text{kbps}$ and target SIR $\varepsilon_1^* = 5.5\text{dB}$, and one E-DCH user class with

adjustable data rates and the same target SIR. The system bandwidth $W = 3.84\text{MHz}$, background thermal noise density $N_0 = -174\text{dBm}$, and PLE (Path Loss Exponent) $\gamma = 4$. To avoid the border effect due to less neighbors for the cells located at the boundary, only the sample values at the central cell are counted.

Fig. 1 illustrates the comparison of mean other-cell interference obtained from simulation and from suggested analytical and enhanced analytical models, while Fig. 2 demonstrates the corresponding standard deviation comparison. The mean number of users in one cell N (i.e. the mean in the spatial homogeneous Poisson process) is assumed to be 9, 15 and 21 respectively, with the ratio between DCH and E-DCH users fixed at 2:1. Since the mean numbers of users assumed in these three scenarios are relatively large, the probabilities of no E-DCH user in one cell are therefore quite small, thus the means of other-cell interference would be similar to each other, and then only one set of results with $N = 15$ is shown. From the figures, we can see the mean values from all the models achieve excellent match, while the standard deviations show slightly greater discrepancy in the case of higher load, which
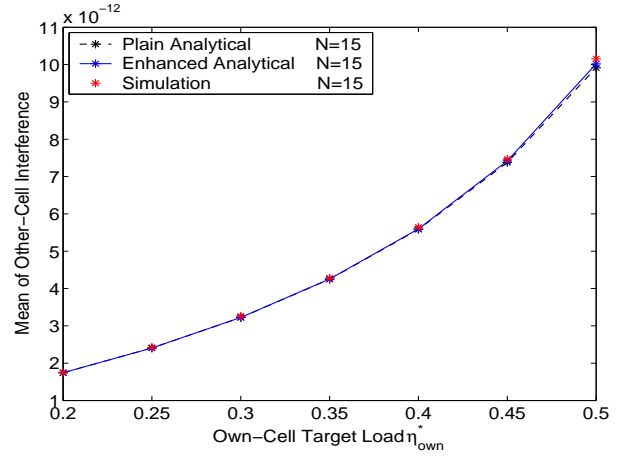

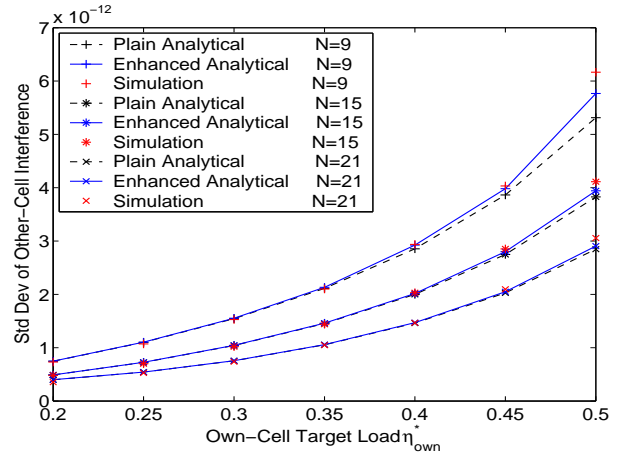Fig. 1. Comparison of mean of other-cell interference

Fig. 2. Comparison of standard deviation of other-cell interference

is due to the mutual independence assumptions made among $\mathcal{I}_{y \to x}^{out}$ as well as between $\mathcal{I}_x^{oc}$ and $\mathcal{F}_{y \to x}$. As one of these independence assumptions ($\mathcal{I}_x^{oc}$ and $\mathcal{F}_{y \to x}$) has been released in the enhanced analytical model (solid line), better accuracy has been achieved in most cases than the plain analytical approximation model (dashed line).

Fig. 3 and 4 demonstrate the same comparisons, but in the cases where the mean DCH user number is fixed at 10 and the mean E-DCH user numbers are quite small. Again excellent matches have been achieved, which implies our model is also valid even there is no E-DCH user in the system, which is quite common in practice. All in all, the good matches in all the scenarios not only verify the validity the log-normal approximation model, but also suggest the possibilities of applying such a model into practical network planning.

VI. CONCLUSION

In this paper, an analytical model have been presented for the characterization of other-cell interference in HSUPA-enabled UMTS networks with distributed RRM. The iterative
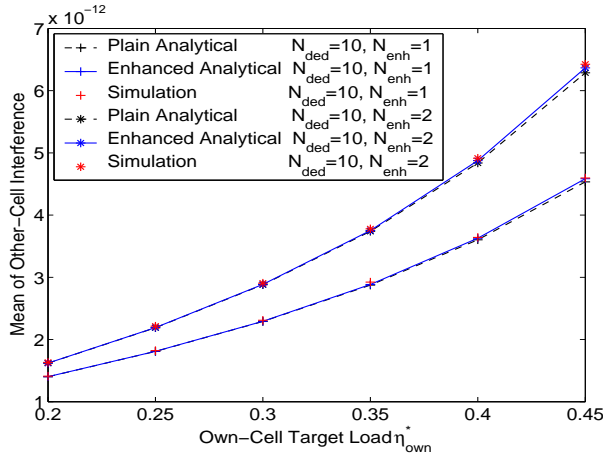

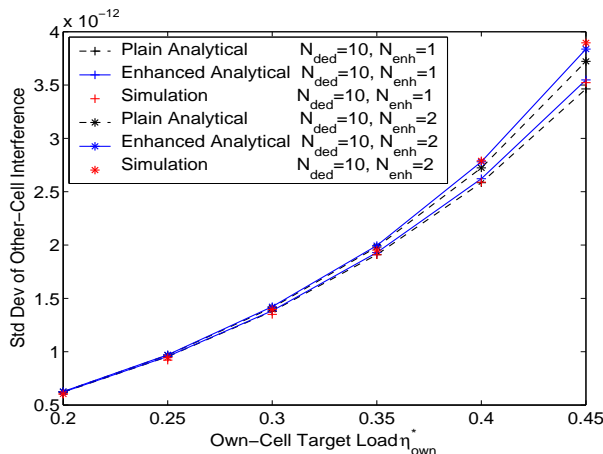Fig. 3. Mean of other-cell interference when E-DCH user number is small

Fig. 4. Std. dev. of other-cell interference when E-DCH user number is small

approach of deriving the PDF of other-cell interference directly where many convolutions involved is firstly described, followed by suggesting an approximation model such that the computation complexity has been greatly reduced and thus numerical tractable. Then, some techniques are introduced to enhance the accuracy of the suggested approximation model.

Both the numerical results from analytical models and the simulation results are illustrated to verify the suggested approximation model. The first and second moments of other-cell interference obtained from analytical models and simulations show excellent match, especially in the lower load region. When the target load increases, the errors over standard deviations slightly go up due to weak independence assumptions made during calculations, which is later compensated by introducing the accuracy enhancement techniques.

In our current analysis, the traffic model assumed for E-DCH users is based on the period of time they are staying in the system. Our future work includes extension of current interference model with more E-DCH traffic models considered. Furthermore, applying such an interference model to the network capacity analysis such as outage probability calculation is quite worth more efforts.

REFERENCES

[1] 3GPP TS 25.308, "High Speed Downlink Packet Access (HSDPA); Overall description."
[2] 3GPP TS 25.309, "FDD Enhanced Uplink; Overall description."
[3] S. Parkvall, J. Peisa, J. Torsner, M. Sågfors, and P. Malm, "WCDMA enhanced uplink - principles and basic operation," in *Proc. IEEE Veh. Technol. Conf.*, vol. 3, Stockholm, Sweden, May 2005, pp. 1411–1415.
[4] D. Staehle, K. Leibnitz, K. Heck, B. Schröder, A. Weller, and P. Tran-Gia, "Approximating the othercell interference distribution in inhomogeneous UMTS networks," in *Proc. IEEE 55th Veh. Technol. Conf.*, vol. 4, Birmingham, USA, May 2002, pp. 1640–1644.
[5] A. Mäder and D. Staehle, "Uplink blocking probabilities in heterogeneous WCDMA networks considering other-cell interference," in *Proc. Southern African Telecommunication Networks & Applications Conference*, South Western Cape, South Africa, Sep. 2004.
[6] T. Liu and D. Everitt, "Analytical approximation of other-cell interference in the uplink of CDMA cellular systems," in *Proc. IEEE 63rd Veh. Technol. Conf.*, vol. 2, Melbourne, Australia, May 2006, pp. 693–697.
[7] A. M. Viterbi and A. J. Viterbi, "Erlang capacity of a power controlled CDMA system," *IEEE J. Sel. Area. Comm.*, vol. 11, no. 6, pp. 892–900, 1993.
[8] J. S. Evans and D. Everitt, "On the teletraffic capacity of CDMA cellular networks," *IEEE T. Veh. Technol.*, vol. 48, no. 1, pp. 153–165, 1999.
[9] T. K. Liu and J. A. Silvester, "Joint admission/congestion control for wireless CDMA systems supporting integrated services," *IEEE J. Sel. Area. Comm.*, vol. 16, no. 6, pp. 845–857, 1998.
[10] S. Anand and A. Chockalingam, "Performance analysis of voice/data cellular CDMA with SIR based admission control," *IEEE J. Sel. Area. Comm.*, vol. 21, no. 10, pp. 1674–1684, 2003.
[11] N. Hegde and E. Altman, "Capacity of multiservice WCDMA networks with variable GoS," *Wireless Networks*, vol. 12, no. 2, pp. 241–253, 2006.
[12] A. Mäder and D. Staehle, "An analytical model for best-effort traffic over the UMTS enhanced uplink," in *Proc. IEEE Veh. Technol. Conf.*, Montréal, Canada, Sep. 2006.
[13] H. Holma and A. Toskala, *WCDMA for UMTS - radio access for third generation mobile communications*. Chichester: John Wiley, 2000.
[14] N. A. Cressie, *Statistics for spatial data*. New York: John Wiley, 1991.
[15] D. Staehle, "Analytic methods for UMTS radio network planning," Ph.D. dissertation, Institute of Computer Science, University of Würzburg, Germany, 2004.